



HAL
open science

Holocene coastal environmental changes and human occupation of the lower Hérault River, southern France

Benoît Devillers, Guénaëlle Bony, Jean-philippe Degeai, Jean Gascó, Thibault Lachenal, Hélène Bruneton, Florian Yung, Hamza Oueslati, Aurelle Thierry

► To cite this version:

Benoît Devillers, Guénaëlle Bony, Jean-philippe Degeai, Jean Gascó, Thibault Lachenal, et al.. Holocene coastal environmental changes and human occupation of the lower Hérault River, southern France. *Quaternary Science Reviews*, 2019, 222, pp.105912. 10.1016/j.quascirev.2019.105912 . halshs-02428711

HAL Id: halshs-02428711

<https://shs.hal.science/halshs-02428711v1>

Submitted on 20 Dec 2021

HAL is a multi-disciplinary open access archive for the deposit and dissemination of scientific research documents, whether they are published or not. The documents may come from teaching and research institutions in France or abroad, or from public or private research centers.

L'archive ouverte pluridisciplinaire **HAL**, est destinée au dépôt et à la diffusion de documents scientifiques de niveau recherche, publiés ou non, émanant des établissements d'enseignement et de recherche français ou étrangers, des laboratoires publics ou privés.



Distributed under a Creative Commons Attribution - NonCommercial 4.0 International License

1 **Holocene coastal environmental changes and human occupation of the lower Hérault**
2 **River, southern France**

3
4 Devillers B.^{1,2}, Bony G.^{1,2}, Degeai J.-P.^{1,2}, Gascò J.^{1,2}, Lachenal T.^{1,2}, Bruneton H.³, Yung F.¹, Oueslati
5 H.¹, Thierry A.¹

6
7 ¹Archéologie des sociétés méditerranéennes, UMR CNRS 5140, Université Paul-Valéry - Montpellier 3, CNRS,
8 MCC, 34000, Montpellier, France

9 ²Labex ARCHIMEDE, ANR-11-LABX-0032-01. Université Paul-Valéry, Montpellier 3, route de Mende, 34199
10 Montpellier cedex 05

11 ³Aix Marseille Univ, CNRS, IRD, INRA, Coll France, CEREGE UMR 7330, Europôle Méditerranéen de l'Arbois,
12 BP80, 13545 Aix-en-Provence, France

13
14 **ABSTRACT**

15 Sea-level rise, human impacts and climate change have deeply affected coastal environments during
16 the Holocene. These forcing factors are studied using the Lower Hérault valley, which constitutes a
17 very representative Mediterranean case study because of (i) its very early, intense and continuous
18 land use since Neolithic times, and (ii) its sensitivity to sea-level rise and Mediterranean climate
19 changes over a relatively small watershed. 34 cores and 61 AMS radiocarbon dates, associated with
20 biological and geochemical analyses, have allowed us to precisely reconstruct the Holocene evolution
21 of the lower valley. Until 6500 cal yr BP, a wave-dominated morphology and retrogradational
22 dynamics were reconstructed. During this phase, ephemeral channels and successive river mouths
23 formed and were rapidly submerged by sea-level rise. The progradational phase began after 6500 cal
24 yr BP, and the alluvial plain gradually built seawards with the formation of a beachridge system
25 outside the valley. Growth of the fertile alluvial plain was coeval with the development of Neolithic
26 agriculture. This alluvial progradation gradually filled the estuary with advances of the mouths,
27 several shallow lagoons and sandbar. The high density of information collected allows us to
28 recognize, for the first time, a pronounced fluvial-dominated deltaic morphology, especially 3000
29 years ago, during the Bronze Age. Lagoonal and coastal shores were continually inhabited. Human
30 land use continually adapted to geomorphological and environmental changes. Around 300 years
31 ago, the delta shifted to a wave-dominated system.

32 **Keywords:**

33 Holocene; Coastal change; Western Mediterranean; Neolithic; Bronze Age; Iron Age; Deltaic
34 evolution; Geomorphology; Ria infilling; Geoarchaeology

35

36 **1 Introduction**

37

38 Between the Last Glacial Maximum (ca. 22 ka BP) and ca. 6 ka BP, sea level rise (SLR) displaced
39 Mediterranean shorelines inland by transgressive dynamics. At a wide scale, the pace and distance of
40 shoreline migration was mainly mediated by the morphology (geomorphological heritage) of the
41 transgressive surfaces which were narrow in active margins and/or mountainous areas (Dubar,
42 1988), or large in passive continental margin (Aloisi et al., 1978; Labaune et al., 2008). At a smaller
43 geographical scale, fluvial valley incision is also an important factor. In such a geomorphological
44 fluvial context, the maximum flooding surface can be more than 13 km from the current coastline
45 (Dubar and Anthony, 1995; Dubar, 2004; Garcia-Garcia, 2005; Devillers, 2008; Traini et al., 2013).

46 These flooded valleys or rias (Goudie, 2018), were subsequently filled by alluvial deposits because of
47 the slowing of sea level rise, attested in almost all of the geological contexts of the Mediterranean
48 from around 7000 BP (Pirazzoli, 1991; Bard et al., 1996; Vacchi et al., 2016), in a context of low
49 accommodation space. The rate and timing of the progradation phase is sensitive to variations in
50 sediment supply, related to human and/or climatic events (Devillers, 2008; Anthony et al., 2014). For
51 large river systems, these dynamics led to deltaic construction from the narrow valley to the open
52 sea (Aloisi, 1986; Stanley and Warne, 1994; Vella et al., 2005; Vött et al., 2006; Amorosi et al., 2004,
53 2013). For smaller valleys with lower sediment supply, the flooded fluvial valley topography (ria) was
54 progressively silted but did not exceed the mouth of the valley as illustrated by the present
55 shorelines of most Mediterranean fluvial embayments (Anthony et al., 2014). Depending on climate,
56 human history and geomorphological heritage, sedimentation in some systems has not reached yet
57 the downstream valley, as for example for some small watersheds in the Northern part of the Black
58 Sea (Dolukhanov et al., 2009).

59 Based on these trends, we can formulate the following hypotheses. During the transgressive period,
60 (between ca. 18 ka BP and 7 ka BP) the retrogradational coastal system track could produce a wave-
61 dominated delta morphology (Galloway, 1975; Anthony, 2015) because of the lack of sedimentation,
62 the great accommodation space and the rapid sea-level rise.

63 During the first progradation phase (before ca. 7 ka BP), the river-dominated delta morphology
64 (Galloway, 1975; Anthony, 2015) was favoured by a low accommodation space in the narrow valley
65 (Homewood et al., 2000). Wave energy was low, because of the distance from the offshore zone,
66 which concentrated sediment deposition near the river mouth (Allen, 1993). It often resulted in a
67 deltaic morphology dominated by fluvial channels and lagoon systems (Fig. 1).

68 During the second progradation phase, siltation shifted to offshore areas, and the accommodation
69 space became more significant, leading to wave-dominated delta morphology. The active delta front
70 was also more exposed to wave energy, dispersing sediments over wider areas (Allen, 1990, 1993;
71 Anthony and Héquette, 2007). Much like the present morphology of deltas, the shorelines were
72 regularized into large concave curves punctuated by the rocky capes. The lagoons were infilled by
73 sediment supply. For these wave-dominated deltas (Galloway, 1975), offshore dynamics were the
74 main geomorphological agent.

75 **Figure 1: Coastal metamorphosis during the Holocene**

76
77 Sediment accumulation of river systems at base level, linked to the relative stability of sea level from
78 7500 cal yr BP (Lambeck and Bard, 2000; Vacchi et al., 2016), led to the formation of fertile soils and
79 a constant freshwater supply. These environmental conditions were conducive to human settlement
80 and to the emergence of structured societies and trades along the coast (Day et al., 2007; Guilaine
81 and Verger, 2008; Garcia and Sourisseau, 2010). Several studies have shown a direct relationship
82 between the development of deltaic areas and the sedentarization of human societies between 8500
83 and 6500 yr BP (Stanley and Warne, 1997; Kennett and Kennett, 2006; Hu et al., 2013). Before 5000
84 yr BP, many archaeological sites were located close to deltaic areas. These rapidly evolving
85 environments were inhabited by societies that derived their livelihood from the agricultural, fisheries
86 and trading potentialities (Fokkens and Harding, 2003; Guilaine, 2003; Brückner et al., 2002, 2005;

87 Devillers, 2008; Bertoncetto et al., 2014). In these areas, the environmental and human dynamics are
88 closely intertwined, in both space and time (Carozza et al., 2012, Brisset et al. 2018).

89 Although our understanding of human-environment interactions and coastal changes in deltaic areas
90 has advanced significantly in recent years, many questions remain and can only be answered by the
91 multiplication of coring. What was the chronology of these changes? Beyond the simple change of
92 shoreline, is the coastal metamorphosis, namely changes in the nature of the coastal environment,
93 could be proved and measured? Were coastal changes observable at human time-scales? How did
94 environmental changes affect the economic and agricultural systems until the Neolithic?

95 The landscape changes at Agde area, due to the construction and evolution of the Hérault deltaic
96 plain, favoured the installation of ancient societies, especially during the early phase of Neolithization
97 in southern France (Guilaine et al., 2007; Briois and Manen, 2009; Guilaine, 2017). But this area also
98 attests to a dense, continuous and rich occupation history for all the archaeological periods of the
99 Bronze Age, Iron Age and Antiquity (Lugand and Bermond, 2002; Ugolini, 2002; Gomez, 2011; Gascò,
100 et al., 2012, 2015). Archaeological remains of these ancient settlements are sporadically detected in
101 the Hérault catchment and on the rocky volcanic promontory of Agde. By contrast, our
102 understanding of the settlement history of the lower Hérault plain is poor due to the significant
103 sediment accumulations in these areas (Ambert *in* Lugand and Bermond, 2002; Ropiot, 2007; Gomez,
104 2011; Gascò et al., 2012, 2015).

105

106 The aim of this paper is to investigate the Holocene geomorphological evolution of the Lower Hérault
107 valley, in order to establish a dynamic model for coastal changes since 10 000 y. BP. The Lower
108 Hérault valley and the Agde area constitute interesting case studies to probe coastal changes in and
109 around archaeological contexts (Garcia, 1995). It could be used as a model for the Holocene
110 morphogenesis and human-society co-evolution.

111

112 To refine the landscape evolution in the Hérault lower valley and improve our understanding of the
113 environmental context of the site of La Motte, a multidisciplinary research project was initiated. The
114 main objectives of this project were notably to determine the extension of the lagoonal-marine
115 domain inside the palaeo-ria, the position of the coastal sandbars and barrier beaches, and the
116 palaeogeography of the floodplain and palaeochannels of the Hérault River. This study is the first one
117 to be undertaken in the Hérault valley, and complements previous research on western
118 Mediterranean deltas and coastal geosystems during the Holocene (Dubar and Anthony, 1995;
119 Blanchemanche et al., 2002; Dubar, 2004; Arnaud-Fassetta, 2003, 2004; Vella et al., 2005; Devillers et
120 al., 2007; Bertoncetto et al., 2014; Faisse et al., 2015; Dolez et al., 2015). The originality of this work is
121 the highly detailed geomorphological evolution provided by numerous cores and the better
122 understanding of the relation between societies and environment in Agde territory. This paper
123 focuses on the palaeogeographical evolution of the lower Hérault valley and is based on the bio-
124 sedimentological study of 36 sedimentary cores from the coastal plain.

125

126 **2 Study area, a Mediterranean coastal floodplain**

127 **2.1 Geomorphic setting**

128 The Hérault River is located on the Languedoc plain, in South of France. It is a Mediterranean coastal
129 river and its source is Mount Aigoual in the Cevennes area. Its geomorphology begins at the end of

130 the Eocene. The Pyrenean-Alpine orogeny created the Villeveyrac syncline, north of the Etang de
131 Thau, and the anticline of Castelnaud-de-Guers, northeast of Nézignan-l'Evêque (Fig. 2), which forms
132 the very large structure of the Hérault valley. After the Late Miocene, a regression associated with
133 the Mediterranean Messinian salinity crisis (Clauzon et al., 1987; Ambert et al., 1998) incised the area
134 between the current Orb (west of the Hérault valley) and Hérault rivers (Ambert et al., 1998; Larue,
135 2009). The discordant Pliocene series shows a succession of marine sediments and continental
136 deposits filling the deeply incised Messinian palaeovalley and exceeding it up to 100 m NGF.

137

138 Volcanic activity occurred in the lower Hérault valley from the late Lower Pleistocene to the early
139 Middle Pleistocene (Berger et al., 1978; Féraud and Campredon, 1983; Gastaud et al., 1983). It was
140 characterized by effusive, strombolian, and hydromagmatic eruptions that respectively created the
141 basaltic plateaus of Agde and Saint-Thibéry, the scoria cones of Mount Saint-Loup and Mount Ramus,
142 and the tuff-ring of Cape d'Agde. The creation of these volcanic landscapes associated with an
143 eustatic lowstand sea level led to a new incision of the present course of the Orb and Hérault valleys.
144 Thereafter, during Pleistocene times, a system of stepped alluvial terraces was deposited over the
145 Pliocene sediments.

146

147 The Holocene sequence is spatially restricted to the coastal area and the active flood plain of the
148 present rivers. Along its lower part beyond Saint-Thibéry, it flows in meanders on the plain. The slope
149 of the river is low, leading to the formation of a low and flat coastal plain from Florensac, as well as a
150 reduction in sediment grain-size (Berger et al., 1978). The low topography also contributes to the
151 development of secondary networks located at the limit of the floodplain, such as the current
152 Ardaillon River (Fig. 2). The Hérault River flows into the Mediterranean, and its watershed is around
153 2550 km². The present average river flow is ca. 50 m³/s, but the river witnesses strong rain storms
154 (the so-called Cevenol events). These strong rainfall events lead to brutal flood events (up to
155 1500m³/s) on the Hérault lower valley (SAGE, 2005). River flow has been significantly mediated by
156 Holocene rapid climate changes (Degeai et al., 2017).

157

158 **Figure 2: Geological map of the lower Hérault region**

159

160 **2.2 Archaeological context and human occupation of the Hérault lower valley**

161 The west of the valley attests to the earliest documented Neolithic settlements in the western
162 Mediterranean, dating to ca. 7600 BP. These sites provide evidence of the exploitation of the
163 environment with new imported farming and crops technics (Manen and Guilaine, 2007; Briois et al.,
164 2009). The impact of these Neolithic societies on the forest cover and soil erosion, consequently, on
165 fluvial sediment supply is attested by pollen (Court-Picon et al., 2010) and geoarchaeological
166 (Devillers and Provansal 2003) analysis. Furthermore, sites suggest the existence of docking and
167 anchorage areas further inland, consistent with the maximum flooding stage of the Languedoc coast
168 (Gascò et al., 2015). The coastal plain and the most fertile lands at this time occupied a small area
169 because of the ending of the transgressive phase.

170 At the beginning of the Bronze Age (ca. 4250 cal yr BP), landscape clearance can be attributed to
171 several small settlements. They probably benefited from the stabilization of mean sea level and the
172 progradation phase which contributed to create a lagoonal system and alluvial plain. Nonetheless,

173 the paleogeography and the coastline, as well as the deltaic, lagoonal and fluvial (i.e. channels)
174 systems are unclear.

175 Until 2011, underwater archaeological surveys undertaken by UMR5140 ASM and IBIS association in
176 the Hérault riverbed led to the discovery of a protohistoric dwelling dating to the late Bronze Age
177 (Bronze final IIIb, between ca. 3000 and 2700 cal yr BP). This archaeological site, called La Motte, is
178 located north of Agde, in the middle part of the coastal plain, at -5 m NGF. The site comprises
179 ceramics and organic deposits, wood-pile alignments and accumulations of basalt blocks, interpreted
180 as a managed lagoon-river bank in the vicinity of the habitat (Gascò et al., 2015). This pile-dwelling
181 settlement lies near lagoonal clay layers and river-mouth deposits, which demonstrate that this
182 Bronze Age settlement was located between a palaeolagoon and a river mouth. Understanding the
183 environmental evolution of deltaic plain is therefore key to contextualizing the archaeological data.
184

185 Downstream, close to the sea, the Cap d'Agde harbour excavation has unearthed many metal objects
186 consistent with human societies (Mazière, 2013). The populations of the end of the Bronze Age have
187 invested the Hérault lower valley and the Mediterranean coastline.
188

189 For the late 7th century BC, the excavation of the Peyrou Necropolis shows the presence of an
190 indigenous community (Fig. 2-3) on the basaltic promontory of Agde. At that time, local people had
191 already established contacts with the Mediterranean world (Ugolini, 2010), as demonstrated by the
192 Greek vases from the necropolis of Peyrou (Nickels et al., 1981; Dedet and Schwaller, 2017). At about
193 4.4 km from the current mouth of the Hérault River, a shipwreck cargo (Garcia, 2002) or more likely
194 votive deposit (Gascó et al., 2012) dated to the 6th century BC was discovered and confirms maritime
195 activity and long-distance trade in the Agatois area.
196

197 The foundation of the ancient Greek city of Agde dates to 550-525 BC. It will remain active until
198 about 50 AD (Nickels et al., 1989; Nickel, 1989; Ugolini, 2002). The city is installed on a volcanic
199 promontory overlooking the left bank of the Hérault River. Lower draught shipwrecks went up the
200 river to trade with the native populations. The location of the Greek harbour is still not known, due
201 to the progradation and avulsions of the Hérault delta, and thus this work could greatly help to find
202 it.
203

204 During the early Roman Empire, Agde became a key town. Numerous sites were mentioned, and
205 trade on the river, related to the export of wine, is attested (Lugand and Bermond, 2002). At this
206 time, the progradation of the Hérault delta led to the infilling of lagoons and an extension of fertile
207 land conducive to human activities. Nonetheless, the environment of the city of Agde is not known
208 during this period.
209

210 **Figure 2: Geological map of the lower Hérault region**

211 **3. Materials and methods**

212 **3.1 Coring**

215 The Holocene palaeoenvironments of the Hérault lower valley have been reconstructed using
216 sedimentological, palaeobiological and chronostratigraphic data. Thirty-four cores were drilled on
217 the alluvial plain, all of them yielding precise stratigraphic information. The lithological, geochemical
218 and biological content were analysed for ten stratigraphic cores. These cores formed a transversal
219 transect to the deltaic plain (Fig. 3). This transect is particularly useful to reconstruct
220 palaeoenvironments of the alluvial plain, and to spatially constrain the palaeo-channels of the
221 Hérault River and its palaeocoastline. The coring campaign was undertaken in April and October 2014
222 using an Atlas Copco Cobra TT percussion corer. The sampling interval depends on the nature of the
223 sediment, and varied between 5 and 10 cm. The multiplication of coring is favored in this work
224 compared to pollen or geophysical approaches for example. Indeed, the large number of coring is the
225 better approach to reach the objective which is to better characterize the environments and the
226 littoral morphology.

227 3.2 Lithological and sedimentological studies

228 In the ASM laboratory (UMR5140 Paul-Valéry Montpellier 3 University) and Geosciences laboratory
229 (Montpellier University), the sediment texture was determined using wet sieving and laser grain
230 sizing with a Beckman Coulter LS13320 Particle Size Analyser (Fig. 4). A Passega diagram was drawn
231 to determine the hydrodynamic conditions of the depositional environments (Passega, 1964). To
232 characterize the depositional environment in relation to the hydrodynamic conditions (i.e. fluvial,
233 coastal, lagoonal environments), we used the grain-size limits observed in similar coastal
234 environments on the Tiber delta (Salomon, 2013). The results are consistent with other
235 palaeoenvironmental markers.

236 3.3. Biological studies

237 The palaeo-ecology of the different environments was probed using species determination of
238 mollusc shells (macrofauna) present in the sedimentary fraction > 2 mm (Fig. 5-7) and ostracodes
239 present in the dry sand fraction > 150 μm . 47 samples were analyzed. 176 specimens of macrofauna
240 covering 10 taxa were picked and identified using the following references: Clanzig (1987), D'Angelo
241 and Garguillo (1978), Doneddu (2005). The ecological groups were defined according to Péres and
242 Picard (1964), a molluscan classification system for Mediterranean species, and on the basis of the
243 salinity gradient. For the ostracodes, 6081 specimens covering 10 taxa were picked and determined.
244 For each sample we normalised the ostracoda density to a standard dry sample weight (10 g). The
245 ecological groups are based on the salinity gradient between freshwater species and brackish species
246 (Salel et al., 2016).

247 3.4 Mineralogical analyses

248 Optical mineralogical analyses of the sand fraction were performed on nine samples of an E-W core
249 transect. The objective was to determine the influence of the Hérault River on depositional
250 environments. Minerals of biotite and muscovite along with clasts of carbonates and Permian
251 sandstones are indicators of the Hérault watershed, whereas quartz, feldspars, pyroxenes,
252 amphiboles, olivines and lithic fragments of granite and metamorphic rocks are more widespread
253 minerals or clasts.

254 3.5 Geochronology

255 The chronological framework is provided by 61 radiocarbon dates performed at Poznan (Poland) and
256 Saclay (France). Dates performed on charcoal and organic matter have been corrected for
257 atmospheric ¹⁴C variations using the calibration curve IntCal13 (Reimer et al., 2013) (Table 1). Marine
258 shells were calibrated using the Marine13 calibration curve (Reimer et al., 2013). For lagoonal species
259 a Δr correction of 245 years was applied (Degeai et al., 2015). Sixty AMS ¹⁴C were produced. Dated
260 samples were rejected in three cases: (i) if a dated coastal shell was collected from sediment of a
261 fluvial or continental environment (which has been determined with post-dating analysis); (ii) if the
262 ¹⁴C result of a marine material was significantly higher than the expected sea level at the time of
263 deposition, indeed a marine organism collected substantially above the sea level of its time can only
264 be reworked; and (iii) if a single date departed significantly from the age-depth model made up of a
265 large group of reliable dating. We assume that these precautions associated with the large number of
266 available dates is the only method to minimize error caused by reworking.

267

268 **Table 1 : AMS 14C radiocarbon date**

269

270 3.6 Facies catalogue

271 The palaeogeographic results are based on two different methods. Different facies were studied in
272 detail in cores A4 and A8 and subsequently extrapolated to other cores in the valley. On the basis of
273 these results, the other cores are summarized and presented on the basis of the depositional
274 environments (Fig. 8). Palaeogeomorphological maps are based on these analyses, the radiocarbon
275 chronology and the interpretation of present floodplain landforms revealed by Lidar DEM mapping
276 (Fig. 3).

277 **4 Results**

278 **4.1 Facies study in the lower Hérault valley: cores A4 and A8**

279

280 Palaeobiological analyses were performed on three cores from the Zone C transect (A11, A4 and A8).
281 A11 and A8 are located at the extremities of the lower valley, on either side of the Hérault river bank
282 (Fig. 4, 5, 6, 7 and 8). The core A11 is also located on the right flank of the Ardaillon river.

283

284 **4.1.1 Core A8:**

285

286 Core A8 Unit A: Facies 1

287 The basal unit (Unit A) between 13 and 15 m depth consists of an accumulation of ca. 70% of brown
288 sands (50% of medium and fine sands and 20% of coarse sands) in a clayey silt matrix. The gravels
289 fraction is virtually absent (Fig. 4). However, the C/M Passega diagram indicates that these sediments
290 were transported by bed load (at the base) to graded suspension with rolling (at the top) (Fig. 4). This
291 depositional environment is characteristic of open high-energy environment. This interpretation is

292 consistent with the grain-size of the C/M image of Passega diagram limits used by Salomon (2013) to
293 determine palaeoenvironments.

294

295 **Figure 4 : Sedimentological analysis of the A1, A3, A4, A8, A11 and A16 cores**

296

297

298 The sand fraction is composed of ca. 15% of minerals derived from the Hérault watershed (ca. 7% of
299 Permian sandstone clasts, 5% of biotite and muscovite, and 3% of carbonates). 85% of sands
300 correspond to minerals like quartz (78%) and to clasts of granite and metamorphic rocks (7%). The
301 presence of minerals from the Hérault river watershed suggests fluvial inputs into this environment.
302 The microfauna is dominated by euryhaline species such as *Loxoconcha elliptica* and *Cyprideis torosa*
303 at very high faunal population densities (Fig. 5). This association is characteristic of lagoonal
304 environments. This is confirmed by the presence of *Loxoconcha tamarindus*, which is present in the
305 sandy silts of the Thau lagoon (Kurc, 1961). *Hydrobia ventrosa* is the only macrofauna species
306 present, attesting to a brackish depositional environment.

307

308 This highly hydrodynamic environment is characterized by fluvial inputs from the Hérault River. The
309 brackish water salinity indicates a distal connection of the lagoon to the sea. The different proxies are
310 consistent with a riverbed in connection with a lagoon.

311

312 **Figure 5: Ostracod analyses of the core A8**

313

314 Core A8 unit B: Facies 2

315 Unit B is located between 13 and 11.8 m depth and is dated at the base to 7819 ±114 cal yr BP (Table
316 1). The sedimentary texture corresponds to silty sands characterised by ca. 15% of medium and fine
317 sands. Coarse sands are virtually absent (Fig. 4-5). The Passega diagram indicates a pure deposit
318 related to uniform suspension transport and a mixed deposit due to uniform suspension with the
319 injection of graded suspension (Fig. 4). This reduction in grain size is typical of a constant and
320 progressive environmental protection. These grain size characteristics evoke the onset of a less
321 hydrodynamic and more protected environment, with only minor inputs of fine sands (Fig. 4-5). Eight
322 ostracoda species with relatively high faunal population densities were identified. The following
323 lagoonal species are dominant: *Cyprideis torosa*, *Loxoconcha elliptica* and *Loxoconcha tamarindus*.
324 These are found in association with the lagoonal species *Cytherois fischeri* and the littoral species
325 *Leptocythere lacertosa* (Fig. 5). This suggests the onset of a calm lagoonal environment in distal
326 connection with the sea. The presence of freshwater species at high faunal densities (*Candona*
327 *neglecta*, *Heterocypris salina*, *Ilyocypris bradyi*; Fig. 5) attests to the presence of a river mouth in a
328 deltaic context. This interpretation is confirmed by some coastal (*Rissoa ventricosa*) and lagoonal
329 (*Hydrobia ventrosa* and *Scrobicularia plana*; Fig. 6) macrofauna. Charophyte gyrogonites are present
330 in abundant quantities (Fig. 5 and 6). They are indicative of fresh to low salinity environments (Soulié-
331 Märsche, 2007) and support the hypothesis of a river mouth with hydro-sedimentological injections
332 in a protected lagoon.

333

334 Core A8 unit C: Facies 3

335 Unit C is located between 11.8 and 9.2 m depth. It consists of an accumulation of silty sand (ca. 20%
336 of medium and fine sand and ca. 10% of coarse sand; Fig. 4-5). Between 11.6 and 10.3 m depth, the
337 sediment comprises an alternation of greyish silty sand with whitish sandy-marls. The sand
338 percentage is higher than in the rest of the unit (ca. 35%). Between 9.8 and 10.1 m depth, the
339 sediment comprises an organic deposit. This peat deposit has been dated to 7494 ± 73 cal yr BP
340 (Table 1). The Passega diagram places the sandy-marl sub-unit in mixed deposit due to uniform
341 suspension with the injection of rolling deposit (Fig. 4). The environment is calm and protected but
342 records some sandy-marl injections. Lagoonal ostracods decrease in favour of freshwater ostracods
343 dominated by *Candona neglecta* and *Heterocypris salina* (Fig. 4). The environment corresponds to a
344 freshwater swamp or a frequently flooded fluvial plain. Macrofauna species point to a hydrodynamic
345 environment (Fig. 6). The presence of *Radix peregra* and *Bithynia* sp. in the sandy-marly sub-unit
346 indicates a running freshwater environment. The specie of *Planorbarius corneus* indicates a stagnant
347 freshwater pond (Fig. 6). In light of these data, unit C comprises a fluvial environment, such as a
348 floodplain or a riverbed margin.

349

350 Core A8 unit D: Facies 4

351 Unit D is located between 9.2 and 6.4 m depth. The sedimentary texture corresponds to silty sand
352 characterised by ca. 15% of medium and fine sand and 5% of coarse sand (Fig. 4-5). The Passega
353 diagram indicate pure uniform suspension deposits and some sedimentary lens corresponded to
354 uniform suspension with injection of graded suspension (Fig. 4). The ostracod diversity is high and
355 lagoonal species reappear with the dominance of *Cyprideis torosa* (Fig. 5). The environment
356 corresponds to a lagoon. The permanence of freshwater ostracods indicates a closed deltaic mouth.
357 The low salinity of this lagoonal environment is attested by Charophyte gyrogonites. *Cerastoderma*
358 *glaucum* and *Scrobicularia plana* are euryhaline species that can tolerate low salinities (D'Angelo and
359 Garguillo, 1978) (Fig. 6). The proxies from this unit are consistent with lagoonal conditions.

360

361 Core A8 units E and F: Facies 3bis

362 These two units show similar sedimentary textures consistent with the accumulation of silts. The
363 medium and fine sand fractions are very low (ca. 10%) (Fig. 4). The Passega diagram shows a pelagic
364 suspension for these two deposits consistent with decantation processes in a very protected
365 environment typical of a filling-up lagoon or alluvial plain (Fig. 5-6). In unit E, the sand fraction
366 comprises residual ostracodes from unit D. The environment is characterised by the same association
367 as unit D but in very low abundance. The lagoonal environment is filled up and progressively
368 transformed into an alluvial plain characterized by freshwater ostracods like *Candona neglecta* (Fig.
369 4). The evolution into an alluvial plain is also marked by terrestrial macrofauna such as *Theba pisana*
370 (Fig. 6). This facies is similar to unit 3. Here, however, this fluvial environment is more distal and
371 decantation processes are dominant. The environment is characteristic of a floodplain.

372

373 **Figure 6: Benthic macrofauna analyses of cores A4 and A8**

374

375 **4.1.2 Core A4:**

376 Core A4 Unit A: Facies 1

377 The basal unit (Unit A) is located between 10.2 and 11 m depth. Like unit A of core A8, it consists of
378 an accumulation of sands (10% of coarse sand and 60 % of medium and fine sand) in a clayey matrix.

379 The main difference is the presence of a ballast fraction (15%) comprising gravels and small pebbles
380 (Fig. 7). The Passega diagram indicates a rolling transport processes (Fig. 4) consistent with a very
381 energetic depositional environment such as the bed load of a river channel. Ostracod faunal densities
382 are low with species such as *Loxoconcha elliptica*, *Loxoconcha tamarindus* and *Leptocythere lacertosa*
383 (Fig. 7). This association is typical of a lagoon in proximity to a fluvial mouth and connected to the
384 sea. The presence of the macrofauna *Hydrobia ventrosa* confirms the existence of a lagoonal
385 environment close to this riverbed (Fig. 7).

386 387 **Figure 7: Ostracod analyses of the core A4** 388

389 Core A4 unit B: Facies 4

390 Between 10.2 and 5.4 m depth, unit B is characterised by a medium and fine silty sand sedimentary
391 texture. Coarse sand and ballast are absent. The base and the top of the unit are marked by an
392 increase in the percentage of sands (ca. 20% vs. ca 10%; Fig. 4 and 6). The Passega diagram indicates
393 a uniform suspension process for the deposition of this unit typical of a relatively calm and protected
394 environment (Fig. 4). The ostracods are relatively diversified. Lagoonal species are present in high
395 abundance. *Cyprideis torosa* is the dominant species, confirming the installation of a lagoonal
396 environment. However, the freshwater species *Heterocypris salina* and the abundance of *Loxoconcha*
397 *elliptica* indicate relatively distal fluvial inputs. The number of coastal species, such as *Leptocythere*
398 *lacertosa*, decreases progressively. This is characteristic of the gradual disconnection of the
399 environment from the sea. Variations in freshwater and lagoonal species (Fig. 6-7) indicate some
400 lateral variations in fluvial inputs into the lagoon environment. Like unit A, *Hydrobia ventrosa*
401 gastropods attest to a brackish lagoonal environment (Fig. 6).

402
403 Core A4 unit C: Facies 2

404 Unit C is located between 5.4 and 4 m depth. It consists of pebbles (25%) and sands (55%) in a clayey
405 silty matrix (Fig. 4 and 7). Like unit A, the Passega diagram indicates a very high-energy rolling
406 transport processes typical of river channel bed load (Fig. 4). *Loxoconcha elliptica*, *L. tamarindus* and
407 some secondary freshwater species like *Candona neglecta* and *Heterocypris salina* attest to a river
408 mouth in a lagoonal environment (*Cyprideis torosa*) connected to the sea (*Leptocythere lacertosa*, *L.*
409 *fabaeformis* and *Cytherois fisheri*). The river mouth hypothesis is also supported by the presence of
410 Hérault River watershed minerals at 25%.

411
412 Core A4 units D and E: Facies 3

413 Like units E and F of core A8, these two units are characterised by the accumulation of silts (90%)
414 (Fig. 6). They correspond to alluvial plain environment and highlight the progradation of the Hérault
415 river.

416 417 **4.1.3 Core A33: Facies 5**

418 Core A33 is almost entirely composed of bedded sand, from coarse to fine grain size. Malacofauna
419 fragments are present in the sand fraction. Gastropods and bivalves are represented by
420 *Cerastoderma glaucum*, *Pavicardium* sp. and *Cerithium vulgatum*. They are consistent with the
421 coastal and lagoonal zones. These layers were deposited in a high-energy coastal zone, such as a
422 sand bar.

423

424 Mineralogical observations

425 Almost all optical mineralogical counts of sand grains indicate a clear origin from the Hérault
426 watershed (Fig. 8). Granite clasts, pyroxene, amphibole, olivine, quartz and feldspar are characteristic
427 minerals and lithic fragments of the area, but Permian sandstone, biotite, muscovite and carbonate
428 grains can clearly be attributed to the mid and upper Hérault valley. A marine origin for these sands
429 can be excluded. Nonetheless, in the lower part of the core A11 (riverbed facies), mineralogical
430 markers from the Hérault watershed are absent. We suggest that this is consistent with sediment
431 deriving from the western tributary of the Hérault.

432

433 **4.1.4 Facies model of the lower Hérault valley sedimentological records**

434 The study of these new cores allows us to build a facies model for the lower Hérault valley (Fig. 8).
435 Facies 1 is composed of coarse sand and gravel and it is related to the fluvial channel. Silts and fine
436 sands are sometimes interbedded in the facies. Facies 2 contains mixed lagoonal and freshwater
437 fauna consistent with a lagoon near a rivermouth or a rivermouth in a lagoonal environment. Facies 3
438 comprises brown silts associated with continental malacofauna and is indicative of a floodplain.
439 Facies 4 is characterized by dark clays and loams associated with coastal and lagoonal macrofauna
440 related to a lagoonal deposit. Facies 5 is made-up of shelly sands that we interpret as a shoreline or
441 beachridge. All these facies compose the cores of this study (figure 8). This allows us to elucidate the
442 geomorphological evolution of the Hérault ria since 8000 years.

443

444 **5 Geomorphological evolution of the lower Hérault valley**

445

446 **5.1 Complex transgressive dynamics**

447 Until ca. 5500 BP, transgressive dynamics are predominant and large lagoonal areas are elucidated in
448 all zones (Fig. 8). In the northern part of the valley, cores A13, A14 and A35 record a relatively stable
449 lagoonal environment between 8500 and <7200 cal yr BP. East of the valley, a fluvial wetland rich in
450 organic deposits began accreting around 8000 cal yr BP. The river mouth moved to the west from
451 8000 to 7000 cal yr BP, as shown by cores A8, A16 and A7 cores (Fig. 8-9). During this general
452 transgressive period in the Hérault valley, delta-like progradation occurred, mediated by the position
453 of the river mouth. These progradation dynamics (Fig. 9) were very restricted, mobile and transitory
454 (ephemeral and successive river-mouth). Remnants of these channels can still be perceived by a
455 linear morphology only revealed by a geomorphological analysis of LIDAR data (Fig. 3).

456

457 These successive fluvial environments were submerged (cores A8, A16, A7, A1, etc.) thereafter,
458 during the maximal flooding period between 7000 and 5000 cal yr BP. (Fig. 8-9). Lagoonal sediments
459 are present in almost all cores (Fig. 8). The lagoonal deposits furthest from the current shoreline are
460 found in cores A19 and A21 (zone A, Fig. 7-8), 11.2 km inland. These constitute the farthest coastal
461 environments known nowadays in the valley and it show the maximum extension of the Hérault
462 palaeolagoonal system. No dates are available for the core A19, but if we assume that the first
463 lagoonal deposits (6 m bsl) are in direct relation with sea-level rise at this depth, this maximum
464 extension could be roughly dated to between 7000-6500 cal yr BP, according to regional sea-level
465 curves (Vella and Provansal, 2005; Vacchi et al., 2016). The main progradation phase began after 6500
466 cal yr BP in the middle of the valley. Beachridges and/or sandbars developed inside the lagoon, due

467 to a slowdown in sea-level rise and the sedimentary inputs from the Hérault River and its tributaries.
468 Until this period, the general morphological shape of this inner delta was concave, even if the river
469 mouth could temporally prograde by siltation into small areas along the sides of the valley, where
470 shallow depths could be more easily infilled.

471

472 Downstream, between the present-day cities of Agde and Vias, a large sandy barrier was elucidated
473 during field surveys and mapped using the LIDAR digital elevation model (Fig. 3). The core A33,
474 undertaken on this beach and dune ridge, is 9 m deep and composed almost entirely of sand. After
475 7500 cal yr BP, the aquatic environments inside the ria were brackish and therefore separated from
476 the sea by a sandy barrier. These data demonstrate that the inner sandy barrier was in place until
477 7500 cal yr BP, between Agde and Vias. This barrier seems to be dynamic and discontinuous.
478 Furthermore, it is known that a beachridge was present on the coast during the last 8000 years at
479 least, located approximately on the current coastline (Court-Picon et al., 2000; Tessier et al., 2000;
480 Raynal et al., 2009; Degeai et al., 2015). Once again, core BSS002KQQF (available online at:
481 <http://infoterre.brgm.fr>) comprises 30 m of sand accumulation and reveals the presence of this
482 beachridge. The beachridge was probably not continuous at this time (Court-Picon et al., 2000;
483 Degeai et al., 2015). These natural barriers were conducive to navigation in a sheltered environment
484 and thus promoted the appearance and dissemination of Neolithic culture in the Western
485 Mediterranean. The Peiro Signado and Pont de Roque-Haute archaeological sites, near Vias, are the
486 oldest Neolithic settlements in the region (Guilaine et al., 2007; Briois and Manen, 2009).

487

488 **5.2 Deltaic progradation**

489 The western route of the Hérault fluvial channel, visible in cores A4 and A3, was gradually or
490 suddenly abandoned for a new channel to the east. Until 3000 cal yr BP, sedimentation from the
491 Hérault river began to build a large floodplain on the western part of the valley (Fig. 8-9), then
492 continued to the east of La Motte, a Bronze Age archaeological site (Gascó et al., 2015). These
493 landscape dynamics isolated a small sub-lagoon in the eastern part of the valley. This large and fertile
494 floodplain was attractive to human activities (navigation, agriculture, fishing) (Gascó et al., 2015) and
495 helps to explain the importance and the long duration of La Motte settlement during this period.

496

497 From 3000 to ca. 1000 cal yr BP, the ria continued to be infilled by alluvial sediments in a lagoonal
498 environment. Progradation dynamics were more rapid on either side of the valley, and driven by the
499 Hérault River on the eastern side and, more slowly, by the Ardaillon tributary on the western side.
500 Cores A30, A32 and the Lidar data (Fig. 3) show the general chronology and morphology of this
501 lagoon, which is on the way to be filled. This lagoon, never described in previous studies, is of
502 significant archaeological importance. Agde promontory is known to have accommodated an Iron
503 Age Greek colony (Nickels et al., 1989; Ugolini *in* Lugand and Bermond, 2002) and such a lagoon
504 would have been key for harbour activities and maritime trade. At this time, the Hérault valley was a
505 major commercial route for the exportation of agricultural products throughout the Western
506 Mediterranean (Garcia, 1995; Mauné, 2002; Ropiot, 2009; Mauné, 2016). Archaeological remains
507 have been mapped around Agde, although no harbour structures have been formally identified
508 (Lugand et Bermond, 2002). Scholars have suggested that the Roman harbour could be close to Luno
509 Pond, Rochelongue beach or near the present Hérault river mouth. This could be reconsidered with
510 the knowledge of new data presented here.

511

512 The silting and infilling dynamics continued during the last evolutionary stage of the lower Hérault
513 valley. Cores A32 and A28 suggest that the lagoon was infilled between 1000 cal yr BP (age of the last
514 lagoonal deposit) and 500 cal yr BP (riverbed dated near Agde). Further downstream, the LIDAR DEM
515 shows a relict depression and abandoned river channel just behind the present coastline (Fig. 3).
516 These landforms are clearly discernible in 18th century maps (Garipuy, 1774; Bourgoïn et al., 1777).
517 Likewise, the river mouth and the Grau are also mapped, supported by the geological map of the
518 area (Berger et al., 1978) and field surveys.

519

520 **6 Discussion**

521 The chronostratigraphic record of the lower Hérault valley provides evidence for 7000 years of a
522 deltaic evolution. The numerous cores have helped to elucidate a detailed image of past coastlines
523 and lagoon morphology. Until the end of the transgressive phase, corresponding to the sea-level rise
524 slowdown, the wave-dominated morphology led to the expansion of lagoonal systems. But this
525 period was also characterized by the formation of several narrow deltaic lobes, which were
526 subsequently submerged in the eastern part of the valley. Coastline are very dynamics, asymmetric
527 and more complex than suggested in previous study or expected by models (Dubar and Anthony,
528 1995; Devillers, 2008; Devillers et al., 2007; 2015; Marriner et al., 2012; Ghilardi et al., 2008; Giaime
529 et al., 2019).

530

531 During the progradation phase, deltaic lobes developed in the middle of the valley from west to east.
532 This was probably because of the difference in sedimentation between this part of the valley, which
533 was a little bit lower in elevation at this time, and the eastern part of the valley, which had already
534 gone through a long phase of fluvial sedimentation. The inner delta lagoon systems were gradually
535 infilled. The palaeoriver channel visible on ancient maps and located in the ancient lagoon is
536 consistent with this evolution.

537

538 Beach ridges are present until at least 7000 cal yr BP and could have two origins. The first is more
539 inland, directly connected to the river system. In this case, the beach ridges could be linked to the
540 displacement of the Hérault river sediments, which were reworked in the lagoon system by floods,
541 currents and wave actions. Gravels found in core A30 support this explanation. Studies have shown
542 that reworked sediment can form beach ridges and/or lagoonal sandbars (Brückner et al., 2017). The
543 second explanation is linked to longshore dynamics as attested along much of the Languedoc coast
544 (Certain et al., 2005; Raynal et al., 2009; Court-Picon et al., 2010).

545

546 These steps in ria evolution were mediated by sea-level change dynamics and sedimentary inputs,
547 which were not linear in space or time. The successive morphological legacies make these
548 geomorphological system dynamics not strictly reversible. The weight of each factor is difficult to
549 quantify precisely. Indeed, each core and its associated proxies yield only a partial image of
550 landscape changes as a whole. Nonetheless, we tentatively quantify the evolution of the surface area
551 of the coastal plain surface inside the lower Hérault valley (Fig. 10a). From the maximum
552 transgressive surface to the present landscape, the coastal plain extends from 5.6 to 43 km². Before
553 6000 cal yr BP, the submerged (or eroded) surface was about 0.7 ha/yr. Thereafter, during the
554 ensuing 6000 years, coastal progradation expanded the plain by around 0.7 ha/yr. This rate was

555 relatively regular except during the Roman period and late antiquity, when it was at 1 ha/yr. At
556 present, it is not possible to compare our results with very high-resolution palaeoclimate data or the
557 detailed land use history of the Hérault watershed. However, several key periods emerge from the
558 data. Deceleration of sea-level rise, between 8000 and 6000 cal yr BP (Stanley, 1995; Flemmings et
559 al., 1998; Vacchi et al., 2016), led to deltaic formation (Stanley and Warne, 1994) around 6000 cal yr
560 BP. The progradation phase in the Hérault valley began slightly earlier, i.e. after 7000 cal yr BP. Very
561 early Neolithization of the area is attested by Peiro Signado and Pont de Roque-Haute archaeological
562 sites, which are the earliest Neolithic settlements known for the Western Mediterranean (Guilaine,
563 2003; Guilaine et al., 2007; Manen and Guilaine, 2007; Briois and Manen, 2009). This early
564 progradation phase could have resulted from accelerated erosion (Devilleers and Provansal, 2003)
565 through Neolithic landscape clearing and agriculture. The progradation phase was mainly controlled
566 by sea-level variations and accelerated by human impacts on local sediment budgets. Moreover, the
567 rapid development of the coastal plain could have contributed to the successful development of the
568 local Neolithic settlements. Another regional high-quality paper have also shown the important
569 relationships between shoreline evolution and archaeological evolution during prehistory (Brisset et
570 al. 2018).

571

572 **Figure 10: Coastal evolution compared to sea-level and archaeological remains**

573

574 A further interesting trend in the data is the acceleration of the progradation phase around 2000 cal
575 yr BP. During the Roman period, strong economic and agricultural development is attested in the
576 Hérault valley (Mauné, 2002, 2016; Ropiot, 2009). This development can be measured by an increase
577 in archaeological sites in the area (Fig. 10c) and an increase in sediment supply resulting from
578 human-induced erosion in the middle Hérault valley (Devilleers and Provansal, 2003). At long time
579 scales, an acceleration in progradation was a corollary of watershed agricultural pressures and
580 erosion.

581

582 **7 Conclusion**

583 This work provides detailed insights into Holocene coastal evolution using chronostratigraphic data
584 and Lidar mapping. The Hérault palaeodeltaic lobes, in both retrogradational or progradational
585 phases, were deposited in a relatively small geographic area. This is in contrast to large deltaic
586 systems such as the Rhone delta where the fossilized coastal forms are more spread out, visible and
587 more easily mapped, and therefore better understood (Aloisi et al., 1978; Panin et al., 1983; Coleman
588 et al., 1980, 1998; Amorosi et al., 2001). This methodological aspect may explain why small
589 morphosedimentary systems in coastal areas have received less research attention. New techniques
590 and approaches (LIDAR, multiplication of coring, high resolution geophysical investigation, etc.) must
591 be used to fill this knowledge gap in the coming decades. To understand Holocene landscape
592 dynamics, we stress the importance of a multidisciplinary approach associating (bio)stratigraphy,
593 geomorphology and archaeology.

594

595 The large number of cores undertaken within the framework of this project has allowed us to
596 elucidate the different stages of Holocene coastal metamorphosis. Until the late Holocene, local
597 deltaic systems were submerged in the eastern part of the valley. The Holocene history of the
598 landscape in the Hérault valley began with a maximum flooding surface around 12 km inland ca. 7000

599 years ago. Its infilling began in the western part of the valley and shifted eastwards until Late Bronze
600 Age at least (ca. 3000 cal yr BP). The non-linearity of coastal landscape evolution inside the ria is
601 confirmed by field data and could be taken into account in future numerical models (Dubar, 2004).

602

603 This landscape evolution must be taken in account to understand the archaeological history of the
604 lower Hérault valley: (i) from a taphonomic point of view; (ii) because of the evolution of the most
605 fertile agricultural lands in relation to coastal retrogradation and progradation from the Neolithic to
606 Roman periods; (iii) for the environmental potentialities of harbours and trade routes through time;
607 (iv) for the changing nature of environmental risks for human societies; and (v) for the relationships
608 between economic systems and changing environments. For these reasons, the lower Hérault valley
609 and the region of Agde is an interesting laboratory to study Holocene human-environment
610 relationships over the long time on sensible coastal geosystems.

611

612 **Acknowledgment**

613 This work is funded by the LABEX ARCHIMEDE (program "Investissement d'Avenir" ANR-11-LABX-
614 0032-01). It is a contribution to the DYLITAG (Labex Archimede) and PCR Evolitt projects (Drac
615 Occitanie) led by B. Devillers. The ARTEMIS program (French ministry of Culture and CNRS) financed
616 the radiocarbon dates. The drill cores and sedimentological analyses were performed by the
617 ArcheoEnvironnement lab facilities (ASM CNRS UMR5140). The AMS ¹⁴C ages were undertaken by the
618 Centre de Datation par le RadioCarbone (CNRS UMR 5138 1, ARTEMIS program), the Centre for
619 Isotope Research of the University of Groningen and the Poznan Radiocarbon Labs. We also thank
620 the Agde council for field access and help, and the Ibis association for underwater archaeology and
621 coring. We are also thankful to undergraduate students from Paul Valéry Montpellier III University
622 for fieldwork assistance and their enthusiasm. We thank Adena, Natura 2000 Lower Hérault valley,
623 the municipality of Agde and landowners for access to coring sites. We thank the anonymous
624 reviewers for their helpful remarks and suggestions.

625

626 **References**

- 627 Allen, J.R. (1990). The formation of coastal peat marshes under an upward tendency of relative sea-
628 level. *Journal of the Geological Society*, 147, 743-745.
- 629 Allen, J.R. (1993). Muddy alluvial coasts of Britain: field criteria for shoreline position and movement
630 in the recent past. *Proceedings of the Geologists' Association*, 104(4), 241-262.
- 631 Aloisi, J.-C. (1986). Sur un modèle de sédimentation deltaïque, contribution à la connaissance des
632 marges passives., Université de Perpignan, Perpignan.
- 633 Aloisi, J.-C., Monaco, A., Thommeret, J., & Thommeret, Y. (1978). Holocene transgression in the Golfe
634 of Lion (southern France) : paleogeographic and palaeobotanic evolution. *Géographie
635 Physique et Quaternaire*, 32, 145-162.
- 636 Ambert, P. (2001). Géologie et géomorphologie des pays de l'étang de Thau et de la basse vallée de
637 l'Hérault. In A.d.l.e.d. Belles-Lettres (Ed.), *Agde et le bassin de Thau 34/2* (pp. 48-57). Paris:
638 C.I.D.
- 639 Ambert, P., Aguilar, J.-P., & Michaux, J. (1998). Évolution géodynamique messino-pliocène en
640 Languedoc central: le paléo-réseau hydrographique de l'Orb et de l'Hérault (sud de la
641 France). *Geodinamica Acta*, 11(2-3), 139-146.
- 642 Amorosi, A., Colalongo, M.L., Fiorini, F., Fusco, F., Pasini, G., Vaiani, S.C., et al. (2004).
643 Palaeogeographic and palaeoclimatic evolution of the Po Plain from 150-ky core records.
644 *Global and Planetary Change*, 40(1-2), 55-78.

- 645 Amorosi, A., & Mili, S. (2001). Late Quaternary deposition architecture of Po and Tevere deltas (Italy)
646 and worldwide comparison with coeval deltaic succession. *Sedimentary Geology*, 144, 357-
647 375.
- 648 Amorosi, A., Rossi, V., & Vella, C. (2013). Stepwise post-glacial transgression in the Rhône Delta area
649 as revealed by high-resolution core data. *Palaeogeography, Palaeoclimatology,*
650 *Palaeoecology*, 374, 314-326.
- 651 Anthony, A. (2015). Wave influence in the construction, shaping and destruction of river deltas: a
652 review. *Marine Geology*, 361, 53-78.
- 653 Anthony, E., & Héquette, A. (2007). The grain-size characterisation of coastal sand from the Somme
654 estuary to Belgium : Sediment sorting processes and mixing in a tide- and storm- dominated
655 setting. *Sedimentary Geology*, 202(3), 369-382.
- 656 Anthony, E.J., Marriner, N., & Morhange, C. (2014). Human influence and the changing
657 geomorphology of Mediterranean deltas and coasts over the last 6000 years: From
658 progradation to destruction phase? *Earth-Science Reviews*, 139, 336-361.
- 659 Bard, E., Hamelin, B., Aamold, M., Montaggioni, L., Cabioch, G., Faure, G., et al. (1996). Deglacial sea-
660 level record from Tahiti corals and timing of global meltwater discharge. *Nature*(382), 241-
661 244.
- 662 Berger, G., Ambert, P., Gèze, B., Aubert, M., Aloisi, J.-C., Got, H., et al. (Cartographer). (1978).
663 Carte Géologique de la France au 1/50 000, Feuille Agde 1040
- 664 Blanchemanche, P., Chabal, L., Jorda, C., & Jung, C. (2002). In J. Burnouf & P. Leveau (Eds.), *Le delta*
665 *du Lez dans tous ses états: quels langages pour quel dialogue?* (pp. 157-174). Paper
666 presented at the *Les fleuves ont tous une histoire*, Aix en Provence. CTHS, Paris.
- 667 Bourguin, J., Dupain-Triel, J.-L., Lande, L., & Thury, C.-F.C.d. (Cartographer). (1777). Cassini map,
668 Feuille 58 Narbonne
- 669 Briois, F., & Manen, C. (2009). In A. Beeching & I. Sénépart (Eds.), *L'habitat Néolithique ancien de*
670 *Peiro Signado à Portiragnes (Hérault)*. (pp. 31-37). Paper presented at the *De la maison au*
671 *village. L'habitat néolithique dans le Sud de la France et Nord-Ouest Méditerranéen*. Acte de
672 la table ronde des 23 et 24 mai 2003., Marseille. Société Préhistorique française.
- 673 Brisset, E., Burjachs, F., Navarro, B.J.B., & Pablo, J.F.-L.d. (2018). Socio-ecological adaptation to Early-
674 Holocene sea-level rise in the western Mediterranean. *Global and Planetary Change*. *Global*
675 *and Planetary Change*, 169, 156-167.
- 676 Brückner, H., Herda, A., Kerschner, M., Müllenhoff, M., & Stock, F. (2017). Life Cycle of estuarine
677 island. From the formation of landlocking of former island in the environs of Miletos and
678 Ephesos in western Asia Minor (Turkey). *Journal of Archaeological Science: Reports*, 12, 876-
679 894.
- 680 Brückner, H., Müllenhoff, M., Handl, M., & Borg, K.V.d. (2002). Holocene landscape evolution of the
681 Büyük Menderes alluvial plain in the environs of Myous and Priene (Western Anatolia,
682 Turkey). *Zeitschrift für Geomorphologie*, 127, 47-65.
- 683 Brückner, H., Vött, A., Schriever, A., & Handl, M. (2005). Holocene delta progradation in the eastern
684 Mediterranean. Case studies in their historical context. *Méditerranée*, 104, 95-106.
- 685 Carozza, J.-M., Micu, C., Mihail, F., & Carozza, L. (2012). Landscape change and archaeological
686 settlements in lower Danube valley and delta from early Neolithic to Chalcolithic time : A
687 review. *Quaternary International*, 261, 21-31.
- 688 Certain, R., Tessier, B., Barusseau, J.-P., Courpa, T., & Pauca, H. (2005). Sedimentary balance and sand
689 stock availability along a littoral system. The case of the western Gulf of Lions littoral prism
690 (France) investigated by very high resolution seismic. *Marine and Petroleum Geology*, 22,
691 889-900.
- 692 Clanzig, S. (1987). *Inventaire des invertébrés d'une lagune méditerranéenne des côtes de France,*
693 *biocénoses et confinement : l'étang de Salse-Leucate (Roussillon)*. Unpublished Thèse de
694 doctorat, Ecole pratique des Hautes Etudes, Montpellier.

695 Clauzon, G., Aguilar, J.-P., & Michaux, J. (1987). Le bassin pliocène du Roussillon (Pyrénées-
696 Orientales, France) : exemple d'évolution géodynamique d'une ria pliocène consecutive à la
697 crise de salinité messinienne. *Comptes-Rendus de l'Académie des Sciences*, 304, 585-590.

698 Coleman, J.M., Roberts, H.H., Murray, S.-P., & Salama, M. (1980). Morphology and dynamic
699 sedimentology of the eastern Nile delta shelf. *Marine Geology*, 41, 325-339.

700 Coleman, J.M., Roberts, H.H., & Stone, G.W. (1998). Mississippi River Delta: an Overview. *Journal of*
701 *Coastal Research*, 14(3), 698-716.

702 Court-Picon, M., Vella, C., Chabal, L., & Bruneton, H. (2010). Paléo-environnements littoraux depuis
703 8000 ans sur la bordure occidentale du Golfe du Lion. *Quaternaire*, 21(1), 43-60.

704 D'Angelo, G., & Gargiullo, S. (1978). Guida alle conchiglie mediterranee, conoscerle cercarle
705 collezionarle. Milan: Fabbri.

706 Day, J.W., Gunn, J.D., Folan, J.W., Yanez-Arancibia, A., & Horton, B.P. (2007). Emergence of complex
707 societies after sea level stabilized. *EOS*, 88, 160-171.

708 Dedet, B., & Schwaller, M. (2017). Grecs en Gaule du sud, tombes de la colonie d'Agathè (Agde,
709 Hérault, IVe-IIe siècle av. J.-C.). Aix en Provence: Errance.

710 Degeai, J.-P., Devillers, B., Blanchemanche, P., Dezileau, L., Oueslati, H., Tillier, M., et al. (2017).
711 Fluvial response to the last holocene rapid climate change in the Northwestern Mediterranean
712 coastland. *Global and Planetary Change*, 152, 176-186.

713 Degeai, J.-P., Devillers, B., Dezileau, L., Oueslati, H., & Bony, G. (2015). Major storm periods and
714 climate forcing in the Western Mediterranean during the Late Holocene. *Quaternary Science*
715 *Reviews*, 129, 37-56.

716 Devillers, B. (2008). Holocene morphogenesis and land use in a semi-arid watershed, The Gialias
717 river, Cyprus. Oxford: British Archaeological Report - Archaeopress.

718 Devillers, B., Excoffon, P., Morhange, C., Bonnet, S., & Bertoncello, D. (2007). Relative sea-level
719 changes and coastal evolution at Forum Julii (Fréjus, Provence). *C.R. Geoscience*, 339, 329-
720 336.

721 Devillers, B., & Provansal, M. (2003). La morphogenèse d'un géosystème cultivé depuis le Néolithique
722 Récent : les petits bassins versants de la moyenne vallée de l'Hérault. *Géomorphologie(2)*,
723 83-98.

724 Devillers, B., Brown, M., & Morhange, C. (2015). Paleo-environmental evolution of the Larnaca Salt
725 Lakes (Cyprus) and the relationship to second millennium BC settlement. *Journal of*
726 *Archaeological Science: Reports*, 1(0), 73-80.

727 Dolez, L., Salel, T., Bruneton, H., Colpo, G., Devillers, B., Lefèvre, D., et al. (2015). Holocene
728 palaeoenvironments of the Bages-Sigean lagoon (France). *Geobios*, 48, 297-308.

729 Dolukhanov, P., Kadurin, S., & Larchenkov, E. (2009). Dynamics of the coastal North Black Sea area in
730 Late Pleistocene and Holocene and early human dispersal. *Quaternary International*, 197, 27-
731 34.

732 Doneddu, M., & Trainito, E. (2005). Conchiglie del Mediterraneo, guida al molluschi conchigliati.
733 Milan: il Castello.

734 Dubar, M. (1988). La série transgressive côtière holocène de la région de Nice, un modèle
735 sédimentaire. *Bulletin de l'Association française pour l'étude du Quaternaire*, 25(1), 11-15.

736 Dubar, M. (2004). L'édification de la plaine deltaïque du Bas Argens (Var, France) durant la
737 Protohistoire et l'Antiquité. Application d'un modèle numérique 2D à l'archéologie.
738 *Méditerranée*, 102, 47-54.

739 Dubar, M., & Anthony, E. (1995). Holocene environmental change and river-mouth sedimentation in
740 the Baie des Anges, French riviera. *Quaternary Research*, 43(3), 329-343.

741 Faisse, C., Devillers, B., Gailledrat, E., & Lefèvre, D. (2015). In Paléogéographie et dynamique du
742 système fluviolagunaire de la Berre (Aude) durant l'Holocène (Vol. Ausonius, pp. 793-806).
743 Paper presented at the 37e congrès de l'AFEAF, Les Gaulois au fil de l'eau, Montpellier.

744 Féraud, G., & Campredon, R. (1983). Geochronological and structural study of Tertiary and
745 Quaternary dikes in southern France and Sardinia: an example of the utilization of dike
746 swarms as paleostress indicators. *Tectonophysics*, 98, 297-325.

747 Fleming, K., Johnston, P., Zwartz, D., Yokoyama, Y., Lambeck, K., & Chapell, J. (1998). Refining the
748 eustatic sea-level curve since the last glacial maximum using far- and intermediate- field
749 sites. *Earth and Planetary Science Letters*, 163, 327-342.

750 Fokkens, H., & Harding, A. (2013). *The Oxford Handbook of European Bronze Age*. Oxford: Oxford
751 University Press.

752 Galloway, W.E. (1975). Process framework for describing the morphologic and stratigraphic evolution
753 deltaic depositional systems. In M.L. Broussard (Ed.), *Deltas* (pp. 87-98). Houston: Houston
754 Geological Society.

755 Garcia, D. (1995). Le territoire d'Agde grecque et l'occupation du sol en Languedoc central durant
756 l'âge du Fer. *Sur les pas des Grecs en Occident*, 137-168.

757 Garcia, D., & Sourisseau, J.-C. (2009). In X. Delestre & H. Marchesi (Eds.), *Les échanges sur le littoral*
758 *de la Gaule méridionale au premier Âge du Fer. Du concept d'hellénisation à celui de*
759 *mediterranéisation* (pp. 237-245). Paper presented at the *Archéologie des rivages*
760 *méditerranéens. 50 ans de recherches*, Arles. Errance.

761 Garcia-Garcia, A., Garcia-Gil, S., & Vilas, F. (2005). Quaternary evolution of the Ria de Vigo, Spain.
762 *Marine Geology*, 220(1-4), 153-179.

763 Garipuy (Cartographer). (1774). *Carte du Canal Royal de Capestang à l'Etang de Thau, 4e partie*

764 Gascó, J., Borja, G., Tourrette, C., Yung, F., Verdier, J.-L., Bouby, L., et al. (2015). In F.O.e.R. Roure
765 (Ed.), *Une occupation lagunaire palafittique aux IXe-VIIIe s. a.C. : La Motte (Agde) au fond du*
766 *fleuve Hérault* (pp. 69-86). Paper presented at the *Les Gaulois au fil de l'eau, Actes du*
767 *XXXVIIe colloque de l'AFEAF, Montpellier*. Bordeaux, Ausonius.

768 Gascó, J., Tourette, C., & Borja, G. (2012). A propos du dépôt de bronze launacien de Rochelongue
769 (Agde, Hérault). *Document d'Archéologie méridionale*, 35(1), 229-237.

770 Gastaud, J., Campredon, R., & Féraud, G. (1983). Les systèmes filoniens des Causses et du Bas
771 Languedoc (Sud de la France) : géochronologie, relations avec les paléocontraintes. *Bulletin*
772 *de la Société Géologique de France*, 25(5), 737-746.

773 Gest'eau. (2005). *Schema d'aménagement et de gestion des eaux du bassin du fleuve Hérault.*
774 *Diagnostic*. Clermont l'Hérault: Syndicat Mixte du Bassin du Fleuve Hérault.

775 Ghilardhi, M., Kunesch, S., Stylias, M., & Fouache, E. (2008). Reconstruction of Mid-Holocene
776 sedimentary environments in the central part of the Thessaloniki Plain (Greece), based on
777 microfaunal identification, magnetic susceptibility and grain-size analyses. *Geomorphology*,
778 97(3-4), 617-630.

779 Giaime, M., Marriner, N., & Morhange, C. (2019). Evolution of ancient harbours in deltaic contexts: A
780 geoarchaeological typology. *Earth-Science Reviews*, 191, 141-167.

781 Gomez, E. (2011). *Agde et son territoire : VIIème siècle-Ier siècle avant Jésus-Christ*. Unpublished
782 *Thèse de Doctorat*, Université de Provence, Aix en Provence.

783 Goudie, A. (2018). Rias: Global distribution and causes. *Earth-Science Reviews*, 177, 425-435.

784 Guilaine, J. (2003). *De la vague à la tombe. La conquête néolithique de la Méditerranée*. Paris: Seuil.

785 Guilaine, J. (2017). A personal view of the neolithisation of the Western Mediterranean. *Quaternary*
786 *International*, Accepted, 15.

787 Guilaine, J., Manen, C., & Vigne, J.-D. (2007). *Pont de Roque-Haute. Nouveaux regards sur la*
788 *Néolithisation de la France méditerranéenne*. Toulouse: Ecole des Hautes Etudes en Sciences
789 *Sociales*.

790 Guilaine, J., & Verger, S. (2008). La Gaule et la Méditerranée. In S.C.e. al. (Ed.), *Contacto cultural*
791 *entre el Mediterraneo y el Atlantico (siglos XII-VIII a.n.e)*. La precolonizacion a debate (pp. 219-
792 238). Madrid: CSIC.

793 Homewood, P.W., Mauriaud, P., & Lafont, F. (2000). Best practices in Sequence Stratigraphy for
794 explorationists and reservoir engineers (Vol. 25). Pau: Elf EP - Editions.

795 Hu, L., Chao, Z., Gu, M., Li, F., Chen, L., Liu, B., et al. (2013). Evidence for a Neolithic Age fire-irrigation
796 paddy cultivation system in the lower Yangtze River Delta, China. *Journal of Archaeological*
797 *Science*, 40, 72-78.

798 Kennett, D., & Kennett, J. (2006). Early state formation in the southern mesopotamia: sea levels
799 shorelines, and climate change. *The Journal of Island and Coastal Archaeology*, 1, 67-99.

800 Labaune, C., Tesson, M., & Gensous, B. (2008). Variability of the transgressive stacking pattern under
801 environmental changes control: Example from the Post-Glacial deposits of the Gulf of Lions
802 inner-shelf, Mediterranean, France. *Continental Shelf Research*, 28, 1138-1152.

803 Lambeck, K., & Bard, E. (2000). Sea-level change along the French Mediterranean coast for the past
804 30 000 years. *Earth and Planetary Science Letters*, 175, 203-222.

805 Larue, J.-P. (2009). Morphodynamic evolution of the Orb River (Languedoc, France): evidence of
806 eustatic, tectonic and climatic controls. *Journal of Quaternary Sciences*, 24(3), 294-310.

807 Lugand, M., & Bermond, I. (2002). Carte archéologique de la Gaule 34-2 : Agde et le Bassin de Thau
808 (Vol. 34-2). Paris: Éditions de la Maison des sciences de l'homme.

809 Manen, C., & Guilaine, J. (2007). Pont de Roque-Haute et le cadre chronologique du Néolithique
810 ancien du Sud de la France. In J. Guilaine, C. Manen & J.-D. Vigne (Eds.), *Nouveaux regards*
811 *sur la néolithisation de la France méditerranéenne*, (pp. 47-49). Toulouse: Archives
812 *d'Écologie préhistorique*.

813 Mauné, S. (2002). In S. Lepetz & V. Matterne (Eds.), *La villa gallo-romaine de Vareilles à Paulhan*
814 *(Hérault, fouille A75) : un centre domanial du Haut-Empire spécialisé dans la viticulture ?*
815 *(Vol. 1, pp. 309-337)*. Paper presented at the *Cultivateurs, éleveurs et artisans dans les*
816 *campagnes gallo-romaines. Matières premières et produits transformés, Actes du VIe*
817 *colloque international d'AGER, Compiègne. Revue Archéologique de Picardie*.

818 Mauné, S. (2016). In C. Besson, B. Triboulot, O. Blin, O.d. Cazanove & P. Van-Ossel (Eds.), *Aux*
819 *frontières des cités de Béziers, Lodève et Nîmes : la moyenne vallée de l'Hérault dans*
820 *l'Antiquité. Développement économique et exploitation des territoires (pp. 507-526)*. Paper
821 presented at the *Franges urbaines et confins territoriaux. La Gaule dans l'Empire, Actes du*
822 *colloque international de Versailles, Versailles. Ausonius Editions*.

823 Mazière, F. (2013). Agde et la basse vallée de l'Hérault de la fin de l'âge du Bronze à l'arrivée des
824 Grecs. In S. Verger & L. Pernet (Eds.), *Une odysée gauloise. Parures de femmes à l'origine*
825 *des premiers échanges entre la Grèce et la Gaule (pp. 36-42)*. Lattes: Musée de Lattes.

826 Nickels, A., Marchand, G., & Schwaller, M. (1989). *La nécropole du premier Age du Fer*. Paris: *Revue*
827 *Archéologique de Narbonnaise*

828 Nickels, A., Pellecuer, C., Raynaud, C., Roux, C., & Adgé, J.-M. (1981). *La nécropole du premier âge du*
829 *Fer d'Agde. Les tombes à importations grecques. MEFRA*, 93(1), 89-127.

830 Panin, N., Panin, S., Herz, N., & Noakes, J.-E. (1983). Radiocarbon dating of Danbe delta deposits.
831 *Quaternary Research*, 19, 249-255.

832 Passega, R. (1964). Grain size representation by CM patterns as a geologic tool. *Journal of*
833 *Sedimentary Research*, 34(4), 830-847.

834 Peres, J.M., & Picard, J. (1964). *Nouveau manuel de bionomie benthique de la mer Méditerranée*.
835 *Marseille: Bulletin des recherches et travaux de la station marine d'Endoume*.

836 Pirazzoli, P.A. (1991). *World atlas of Holocene sea level changes (Vol. 58)*. Amsterdam: Elsevier.

837 Raynal, O., Bouchette, F., Certain, R., Séranne, M., Dezileau, L., Sabatier, P., et al. (2009). Control of
838 alongshore-oriented sand spits on the dynamics of a wave-dominated coastal system
839 (Holocene deposits, northern Gulf of Lions, France). *Marine Geology*, 264(3-4), 242-257.

840 Reimer, P., Bard, E., Bayliss, A., Beck, W., Blackwell, P.G., Ramsey, C.B., et al. (2013). IntCal13 and
841 Marine13 radiocarbon age calibration curves 0–50,000 years cal BP. *Radiocarbon*, 55(4),
842 1869–1887.

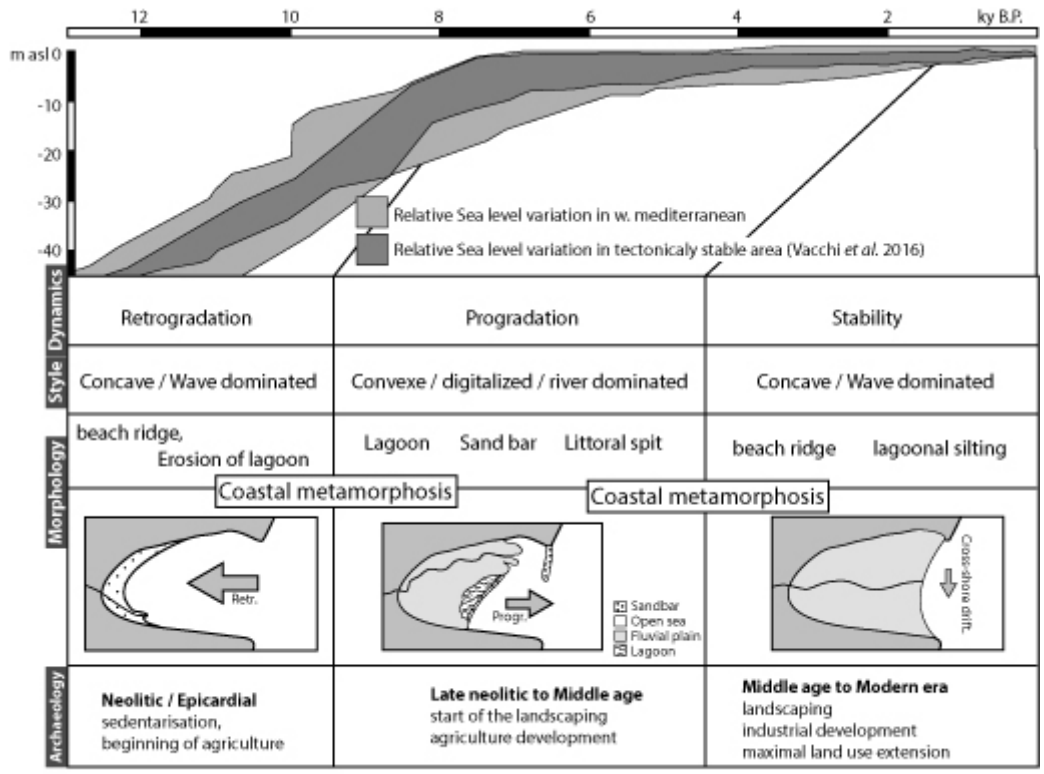
- 843 Ropiot, V. (2009). Peuplement et circulation dans les bassins fluviaux du Languedoc occidental, du
844 Roussillon et de l'Ampourdan du IX^e s. au début du II^e s. av. n. è., Université de Franche-
845 Comté, Besançon.
- 846 Salel, T., Bruneton, H., & Lefèvre, D. (2016). article Ostracods and environmental variability in lagoons
847 and deltas along the north-western Mediterranean coast (Gulf of Lions, France and Ebro
848 delta, Spain). *Revue de micropaléontologie*, 59, 425-444.
- 849 Salomon, F. (2013). Géoarchéologie du delta du Tibre : Evolution géomorphologique holocène et
850 contraintes hydrosédimentaires dans le système Ostie-Portu. Université Lumière Lyon 2,
851 Lyon.
- 852 Soulié-Märsche, I., Benkaddour, A., Khiati, N.E., & Gemayel, P. (2008). Charophytes, indicators of
853 paleobathymetry of lake Tigalmamine (Middle Atlas, Morocco). *Geobios*, 41(3), 435-444.
- 854 Stanley, D. (1995). A global sea-level curve for the late Quaternary: the impossible dream? *Marine*
855 *Geology*, 125, 1-6.
- 856 Stanley, D., & Warne, A. (1994). Worldwide initiation of Holocene marine deltas by deceleration of
857 sea-level rise. *Science*(265), 228-231.
- 858 Tessier, B., Certain, R., Barusseau, J.-P., & Henriot, J.-P. (2000). Évolution historique du prisme littoral
859 du lido de l'étang de Thau (Sète, Sud-Est de la France). Mise en évidence par sismique
860 réflexion très haute résolution. *Comptes Rendus de l'Académie des Sciences*, 331(11), 709-
861 716.
- 862 Traini, C., Menier, D., Proust, J.N., & Sorrel, P. (2013). Transgressive systems tract of a ria-type
863 estuary: The Late Holocene Vilaine River drowned valley (France). *Marine Geology*, 337, 140-
864 155.
- 865 Ugolini, D. (2010). Présences étrangères méditerranéennes sur la côte du Languedoc-Roussillon
866 durant l'âge du Fer : de la fréquentation commerciale aux implantations durables. *Pallas*, 84,
867 83-110.
- 868 Ugolini, D., Olive, C., & Grimal, J. (2002). Agatha, Agde (Hérault). In J.-L. Fiches (Ed.), *LEs*
869 *agglomérations gallo-romaines en Languedoc-Roussillon (P.C.R. 1993-1999) (Vol. 13, pp. 346-*
870 *370)*. Lattes: Monographie d'Archéologie Méditerranéenne.
- 871 Vacchi, M., Marriner, N., Morhange, C., Spada, G., Fontana, A., & Rovere, A. (2016). Multiproxy
872 assessment of Holocene relative sea-level changes in the western Mediterranean: Sea-level
873 variability and improvements in the definition of the isostatic signal. *Earth-Science Reviews*,
874 155, 172-187.
- 875 Vella, C., Fleury, J., Raccasi, G., Provansal, M., Sabatier, F., & Bourcier, M. (2005). Evolution of the
876 Rhône delta plain in the Holocene. *Marine Geology*(222-223), 235-265.
- 877 Vött, A., Brückner, H., Schriever, A., Luther, J., Handl, M., & Borg, K.V.d. (2006). Holocene
878 paleogeographies of the Palairos coastal plain (Arkarnania, northwest Greece) and their
879 geoarchaeological implications. *Geoarchaeology*, 21(7), 649-664.

880

881

882 **Figures**

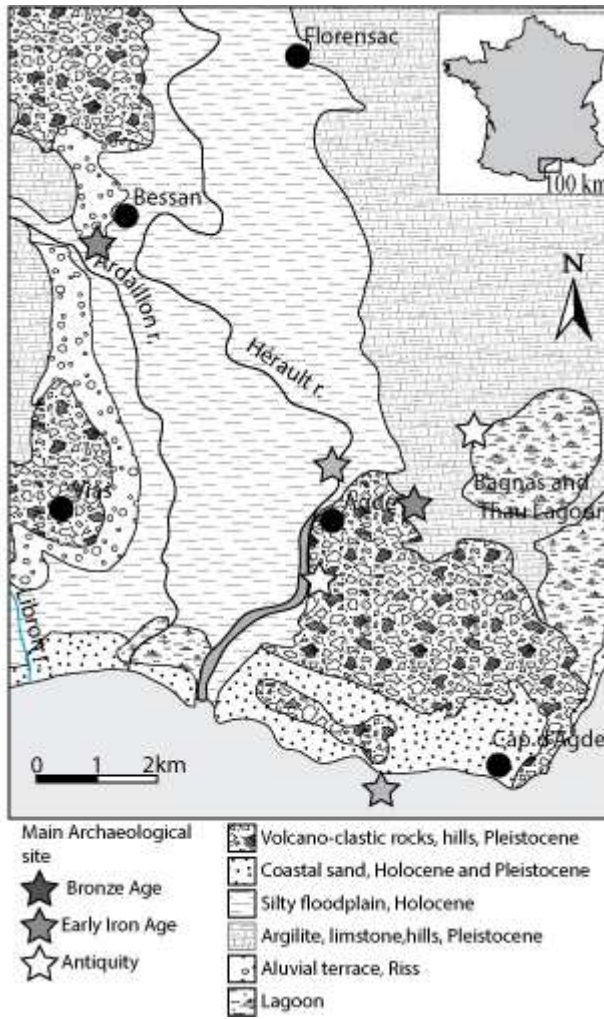
883 Figure 1: Coastal metamorphosis during the Holocene



884
885

886

887 Figure 2: Geological map of the lower Hérault region

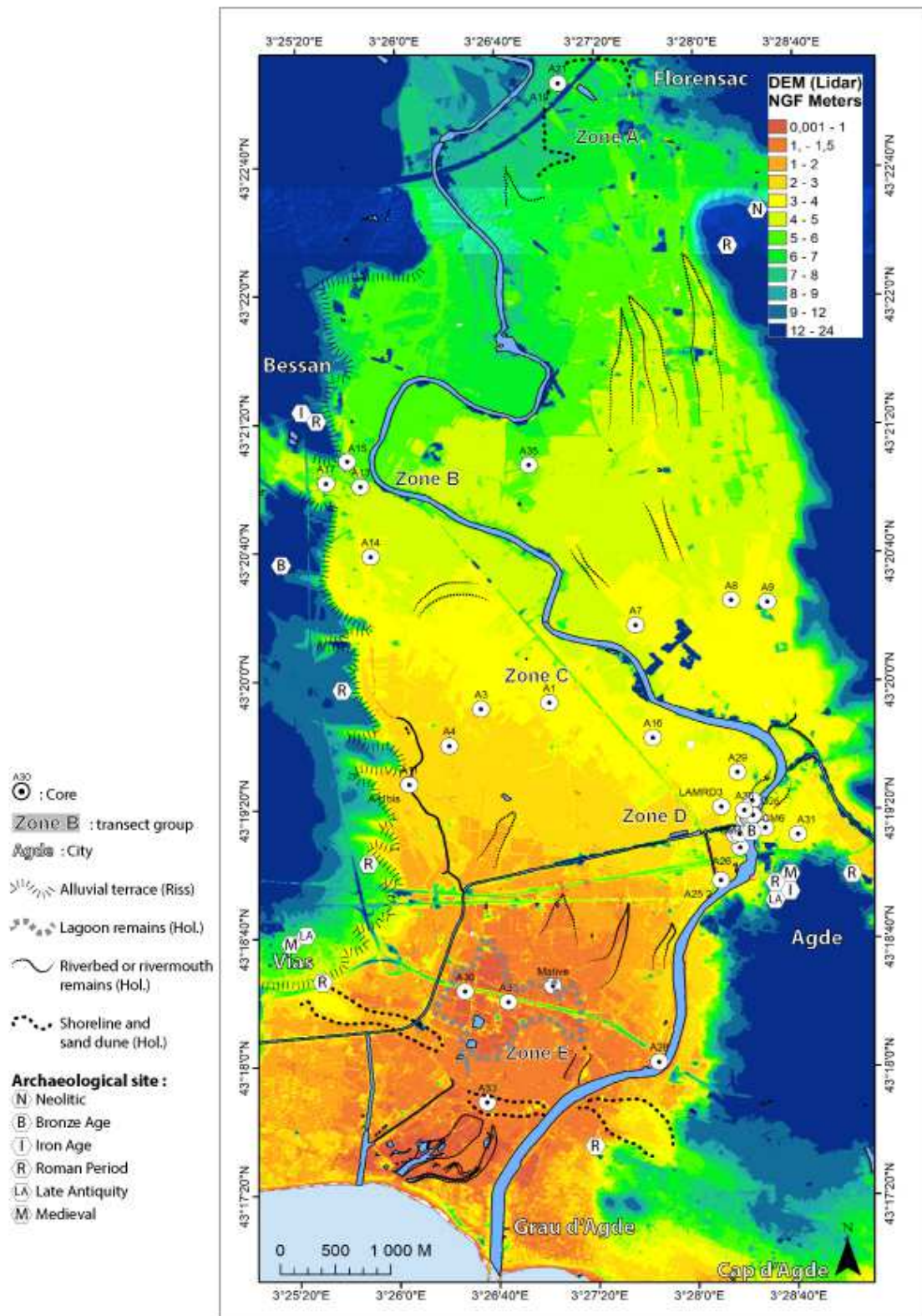


888

889

890

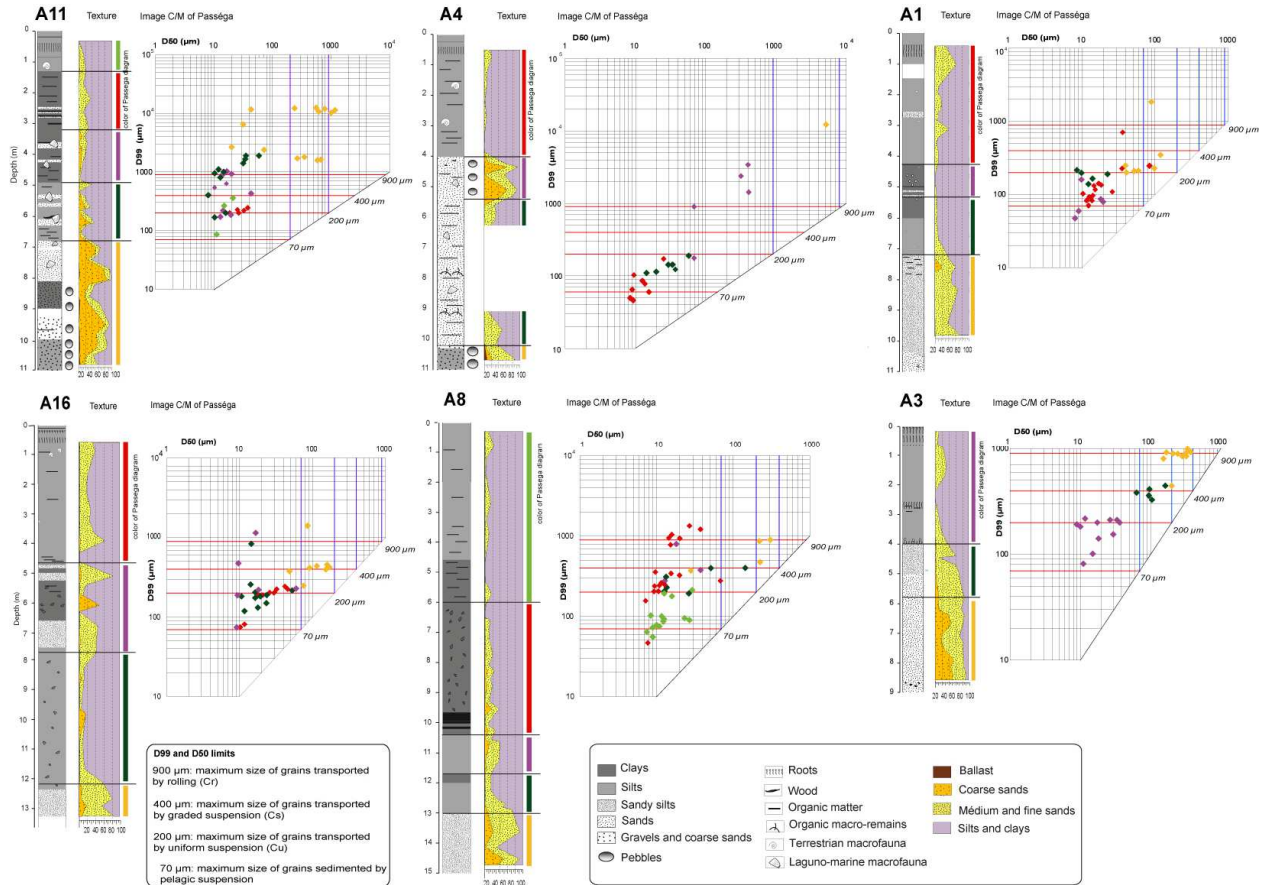
891 Figure 3: Lidar, morphological and archaeological map of the lower Hérault valley



892

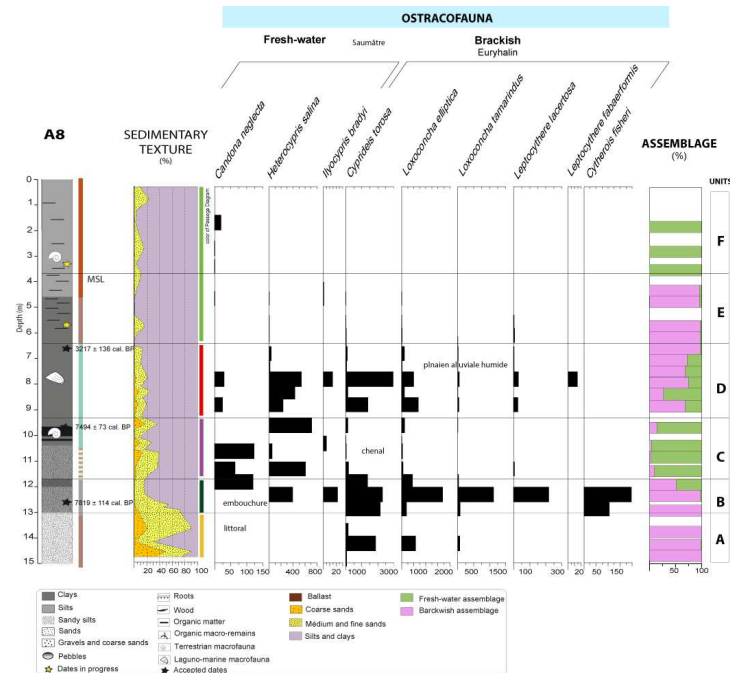
893

894 Figure 4: Sedimentological analysis of the A1, A3, A4, A8, A11 and A16 cores



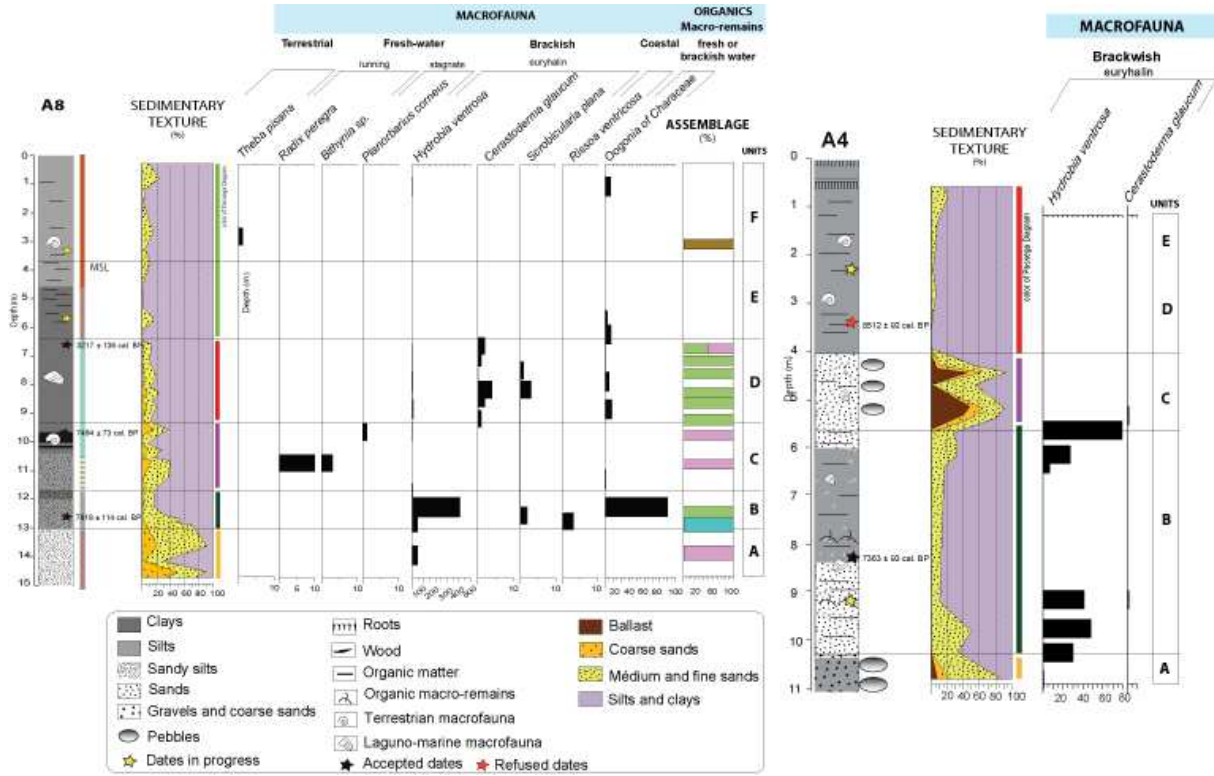
895
896
897
898

Figure 5: Ostracod analyses of the core A8



899
900
901

902 Figure 6: Benthic macrofauna analyses of cores A4 and A8



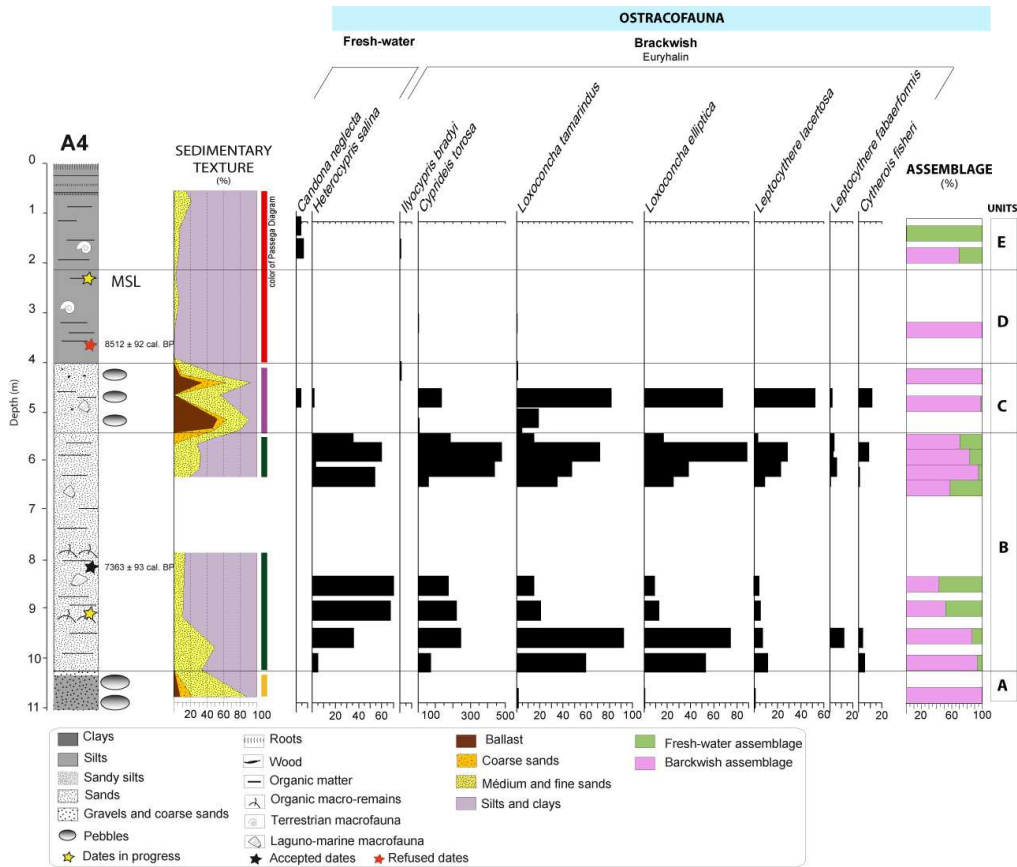
903

904

905

906

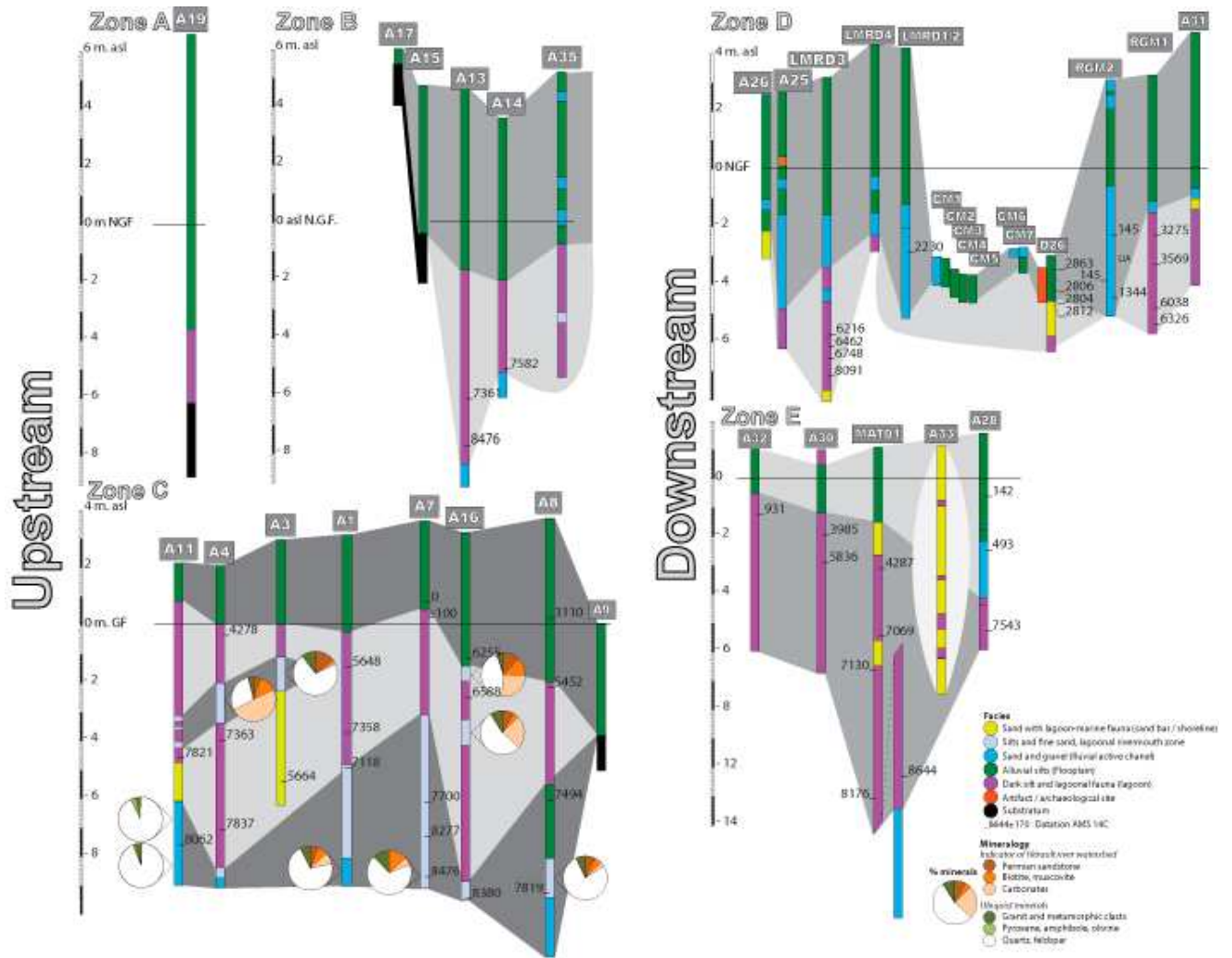
Figure 7: Ostracod analyses of the core A4



907

908

909 Figure 8: Facies distribution of the Hérault's fluvio-lagoonal sedimentary body

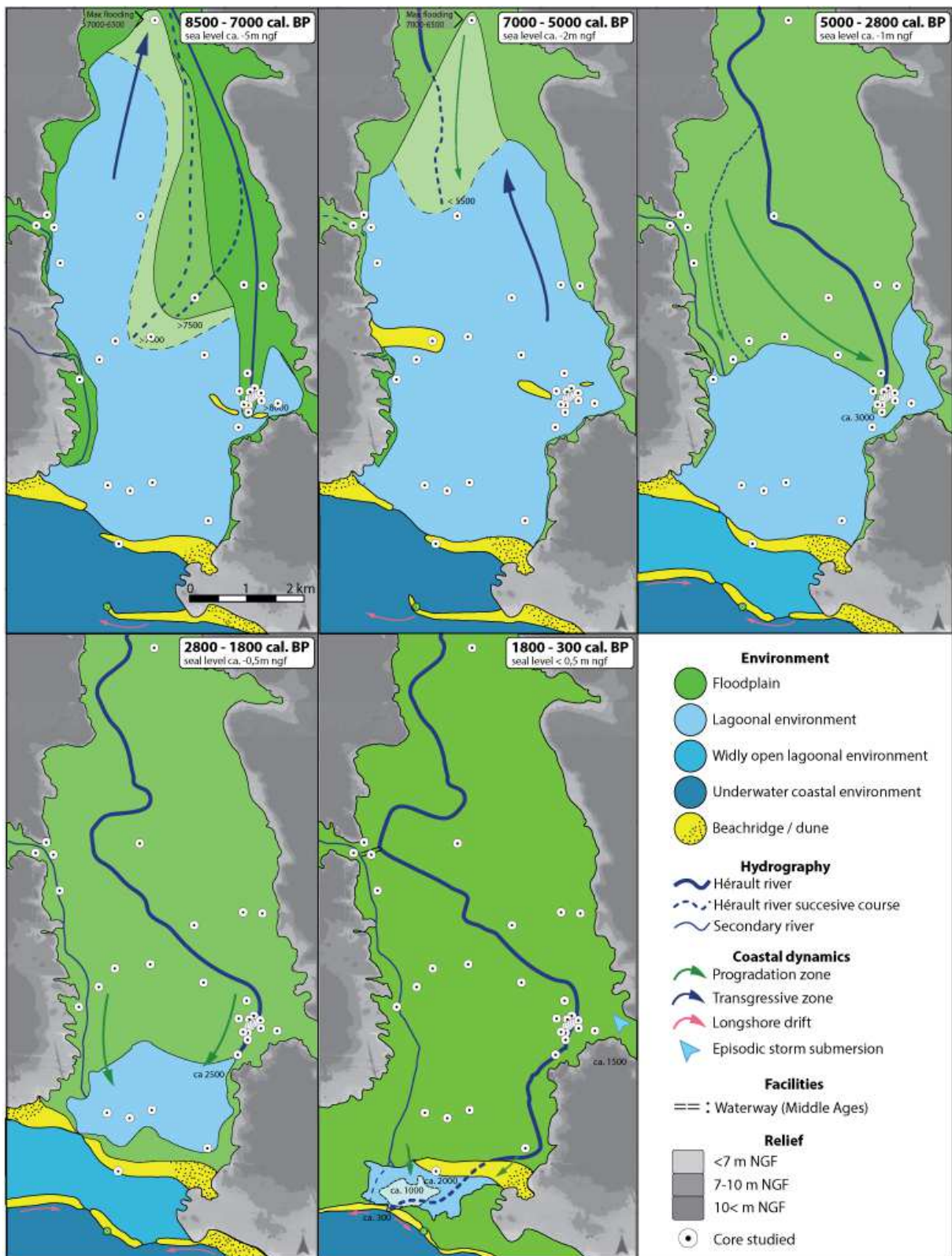


910

911

912

913 Figure 9: Holocene geomorphological evolution of the lower Hérault valley

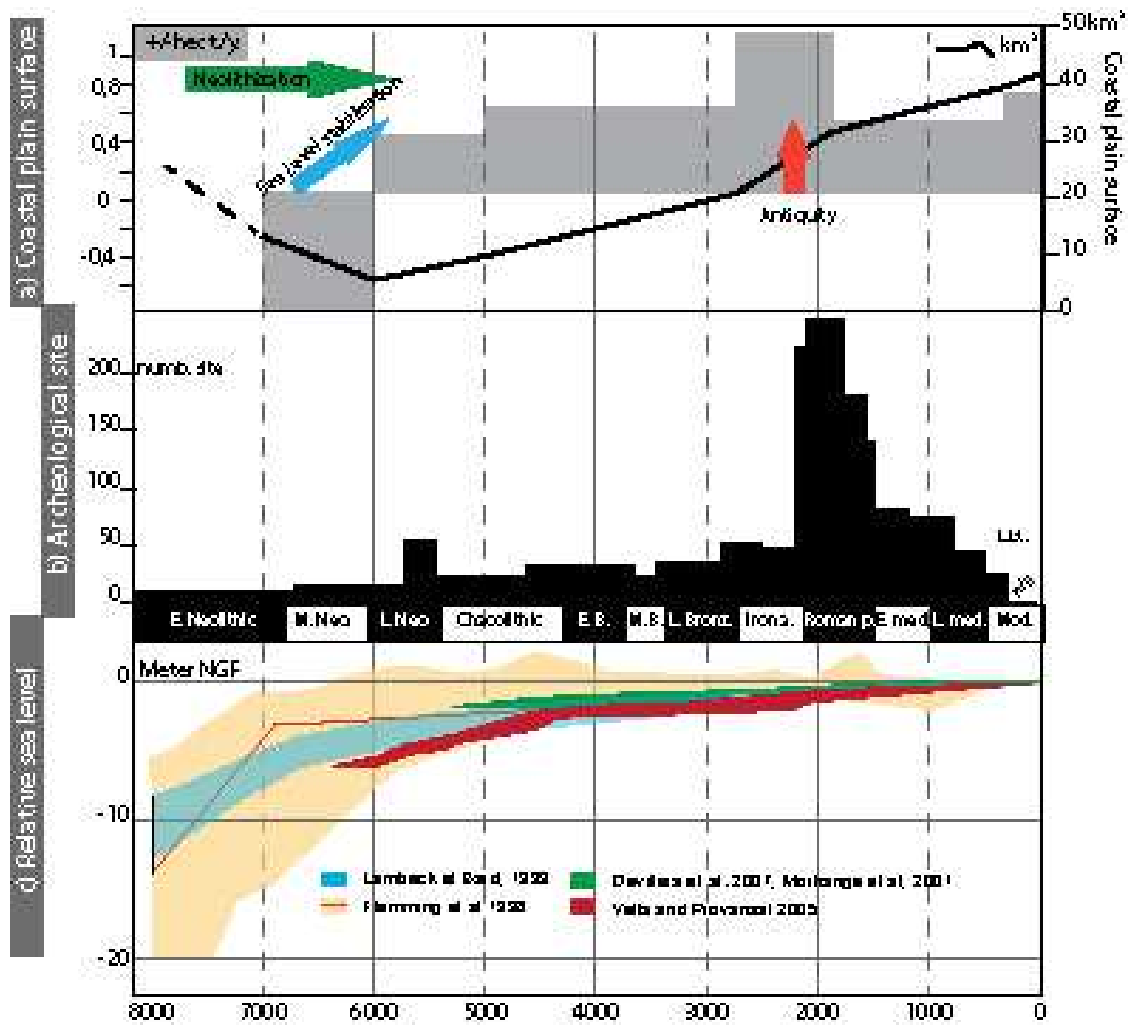


914

915

916

917 Figure 10: Coastal evolution compared to sea-level and archaeological remains



918

919

920